J|A|C|S
ARTICLES
Published on Web 03/16/2007

Large Impact of Particle Size on Insertion Reactions. A Case for Anatase Li_xTiO_2

Marnix Wagemaker,* Wouter J. H. Borghols, and Fokko M. Mulder*

Contribution from the Department of Radiation, Radionuclides and Reactors, Faculty of Applied Sciences, Delft University of Technology, Mekelweg 15, 2629 JB Delft, The Netherlands

Received October 30, 2006; E-mail: m.wagemaker@tudelft.nl; f.m.mulder@tudelft.nl

Abstract: Insertion reactions are of key importance for Li ion and hydrogen storage materials and energy storage devices. The particle size dependence of insertion reactions has been investigated for lithiated anatase TiO_2, revealing progressively increasing Li capacity and Li-ion solubility for decreasing particle sizes, strongly deviating from the expected Li-rich and Li-poor phase separation as occurs in the bulk material. The phase diagram alters significantly, changing the materials properties already at sizes as large as 40 nm. A rationale is found in the surface strain that occurs between the different intercalated phases, which becomes energetically too costly in small particles. In particular the observed particle size-induced solid solution behavior is expected to have fundamental and practical implications for two-phase lithium or hydrogen insertion reactions.

Introduction

Energy storage in the form of Li-ion batteries and H storage requires insertion of Li and H, respectively, into host materials. In order to improve the kinetics of such storage reactions, nanostructuring of the materials has proven to be a promising strategy by shortening the diffusion paths. Additionally, nanostructuring has dramatic effects on the intrinsic material properties, influencing both ionic and electronic charge transport relevant in electrochemical processes.[1−3] Numerous electrochemical studies may indicate also that the thermodynamics of insertion is affected by the crystal particle size.[4−7] For instance the absence of sharp voltage plateaus in multiphase reactions in nanocrystalline matter suggests enhanced solid solution behavior.[4] Here we show systematic and unambiguous structural data that allows fundamental understanding of the impact of particle size on the thermodynamics of insertion. Anatase TiO_2 is a typical lithium insertion compound, showing strong particle size-dependent electrochemistry and insertion capacity,[6,8−13] hence offering an excellent base for the understanding of the effect of nanosizing on insertion reactions. This provided the motivation to embark on a particle size-dependent (7−120 nm) neutron diffraction study (using the sensitivity of neutrons to Li) of Li insertion in anatase TiO_2.

Methods

Synthesis. Anatase TiO_2 (+99%) single crystalline particles with different sizes were obtained from Aldrich: 7 ± 1 and 120 ± 20 nm, NanoAmor: 15 ± 2 nm, Tronox: 23 ± 4 nm, NanoAltair: 40 ± 5 nm. The sizes were determined from the X-ray and neutron diffraction data (analysis of the line-broadening due to the crystallite size) and were consistent with the sizes observed with transmission electron microscopy (TEM). Lithiated materials were prepared by chemical insertion of the vacuum oven-dried TiO_2 powders with *n*-butyllithium[14] (1.6 M, Aldrich). The TiO_2 powders were dispersed in hexane (anhydrous 95+%, Aldrich), and the *n*-butyllithium was added slowly while stirring the diluted mixture, which guarantees homogeneous lithiation of the material. For each crystal particle size, four to five compositions were obtained with different amounts of *n*-butyllithium to form Li_xTiO_2 with overall compositions of $x = 0$, 0.12, 0.4, 0.8*, and a maximum composition which depended on the crystal particle size (* only for crystal particle sizes that allowed the insertion of this

(1) Sata, N.; Eberman, K.; Eberl, K.; Maier, J. Mesoscopic fast ion conduction in nanometre-scale planar heterostructures. *Nature* **2000**, *408* (6815), 946−949.
(2) Maier, J. Defect chemistry and ion transport in nanostructured materials - Part, II. Aspects of nanoionics. *Solid State Ionics* **2003**, *157* (1−4), 327−334.
(3) Maier, J. Nanoionics: ion transport and electrochemical storage in confined systems. *Nat. Mater.* **2005**, *4* (11), 805−815.
(4) Sudant, G.; Baudrin, E.; Larcher, D.; Tarascon, J. M. Electrochemical lithium reactivity with nanotextured anatase-type TiO_2. *J. Mater. Chem.* **2005**, *15* (12), 1263−1269.
(5) Hu, Y. S.; Kienle, L.; Guo, Y. G.; Maier, J. High lithium electroactivity of nanometer-sized rutile TiO_2. *Adv. Mater.* **2006**, *18* (11), 1421−+.
(6) Kavan, L.; Kalbac, M.; Zukalova, M.; Exnar, I.; Lorenzen, V.; Nesper, R.; Graetzel, M. Lithium storage in nanostructured TiO_2 made by hydrothermal growth. *Chem. Mater.* **2004**, *16* (3), 477−485.
(7) Kavan, L.; Prochazka, J.; Spitler, T. M.; Kalbac, M.; Zukalova, M. T.; Drezen, T.; Gratzel, M. Li insertion into $Li_4Ti_5O_{12}$ p(Spinel) - Charge capability vs. particle size in thin-film electrodes. *J. Electrochem. Soc.* **2003**, *150* (7), A1000−A1007.
(8) Ohzuku, T.; Hirai, T. An Electrochromic Display Based on Titanium-Dioxide. *Electrochim. Acta* **1982**, *27* (9), 1263−1266.
(9) Bonino, F.; Busani, L.; Lazzari, M.; Manstretta, M.; Rivolta, B.; Scrosati, B. Anatase as a Cathode Material in Lithium-Organic Electrolyte Rechargeable Batteries. *J. Power Sources* **1981**, *6* (3), 261−270.
(10) Murphy, D. W.; Greenblatt, M.; Zahurak, S. M.; Cava, R. J.; Waszczak, J. V.; Hull, G. W.; Hutton, R. S. Lithium Insertion in Anatase - a New Route to the Spinel $LiTi_2O_4$. *Rev. Chim. Miner.* **1982**, *19* (4−5), 441−449.
(11) Cava, R. J.; Murphy, D. W.; Zahurak, S.; Santoro, A.; Roth, R. S. The Crystal-Structures of the Lithium-Inserted Metal-Oxides $Li_{0.5}TiO_2$ Anatase, $LiTi_2O_4$ Spinel, and $Li_2Ti_2O_4$. *J. Solid State Chem.* **1984**, *53* (1), 64−75.
(12) Wagemaker, M.; Kearley, G. J.; van Well, A. A.; Mutka, H.; Mulder, F. M. Multiple li positions inside oxygen octahedra in lithiated TiO_2 anatase. *J. Am. Chem. Soc.* **2003**, *125* (3), 840−848.
(13) Luca, V.; Hanley, T. L.; Roberts, N. K.; Howe, R. F. NMR and X-ray absorption study of lithium intercalation in micro- and nanocrystalline anatase. *Chem. Mater.* **1999**, *11* (8), 2089−2102.
(14) Whittingham, M. S.; Dines, M. B. Normal-Butyllithium - Effective, General Cathode Screening Agent. *J. Electrochem. Soc.* **1977**, *124* (9), 1387−1388.

amount). If less than the maximum capacity of lithium is introduced to the TiO_2 powders in hexane, all the lithium is inserted since *n*-butyllithium (with a potential of 1 V against lithium) reacts efficiently, as is illustrated by the rapid change of color of the powder (white to blue). After 3 days of stirring, the samples were filtered, washed with hexane, and dried. All sample preparations were carried out in an argon atmosphere glove box to prevent reactions of Li with air. After preparation, the samples were subjected to wet-chemical inductively coupled plasma spectroscopy (ICP) analysis to check the overall composition (ratio Li/Ti). These results, shown in Figure 3(a), are consistent with the Li fractions obtained with neutron diffraction, shown in the same figure. To check that the lithiation procedure leads to equilibrium systems, a few pellets were prepared from the nanomaterials, including 5% carbon black to ensure electrical contact. These pellets were chemically lithiated by *n*-butyllithium and immersed in 1 M $LiCl_4$ electrolyte with a 1:2 ratio of ethylene carbonate/propylene carbonate solvent (Honeywell) to provide ionic contact. Pellets were allowed to relax before diffraction experiments were performed. The results were the same as for the directly intercalated powder materials, proving that also the latter materials were in equilibrium.

Neutron Diffraction. The unlithiated starting materials were characterized with X-ray diffraction. For lithiated samples, neutron diffraction is preferred over X-ray diffraction because of its sensitivity to lithium. The room-temperature neutron diffraction measurements were performed at POLARIS, the medium resolution high-intensity time-of-flight (TOF) diffractometer at the ISIS pulsed neutron source (Rutherford Appleton Laboratory, U.K.). POLARIS is equipped with 434 detectors in four banks covering angles between approximately 160° (backward scattering) and 13° (forward scattering). The neutron diffraction samples were loaded in an argon atmosphere into airtight vanadium sample containers sealed with indium O-rings. The resulting neutron diffraction patterns were refined using the Rietveld method implemented in GSAS.[15] Besides the atomic and lattice parameters, the absorption, and line-broadening parameters, the crystal phase domain fractions and background were fitted. The neutron diffraction line broadening from the fits gives direct information on the crystal domain sizes.

Results and Discussion

In Figure 1(a) neutron diffraction data are shown for the different particle sizes subjected to an overload of butyllithium, hence leading to the maximum lithium composition(s) (equivalent to electrochemical charging at 1 V versus Li metal). As expected, the line-width of the reflections increases for smaller particles as a result of crystal size broadening.

The pristine crystallite particle sizes deduced from the line broadening are consistent with what is observed with TEM. Detailed Rietveld refinement shows that the 120 nm particles fully transform from the initial anatase phase (space-group *I*41/*amd*, $a = b \neq c$) to the expected orthorhombic Li-titanate structure (space group *Imma*, $a \neq b \neq c$) consistent with lithiated microsized particles.[11,12] More surprisingly, additional reflections are observed in the nanomaterials, which could be indexed with the same structure as the pristine anatase TiO_2 (space group *I*41/*amd*, $a = b \neq c$) albeit with very different lattice parameters as given in Table 1. Rietveld refinement of this phase indicates a composition Li_1TiO_2, hosting considerably more Li than the microsized material ($Li_{\sim 0.55}TiO_2$). Interestingly, 7 nm particles can be completely converted toward the newly found Li_1TiO_2 phase, whereas larger particles are systematically less converted, which makes that the maximum obtainable lithium load depends systematically on the particle size.

(15) Williams, W. G.; Ibberson, R. M.; Day, P.; Enderby, J. E. GEM - General Materials Diffractometer at ISIS. *Phys. B* **1997**, *241*, 234−236.

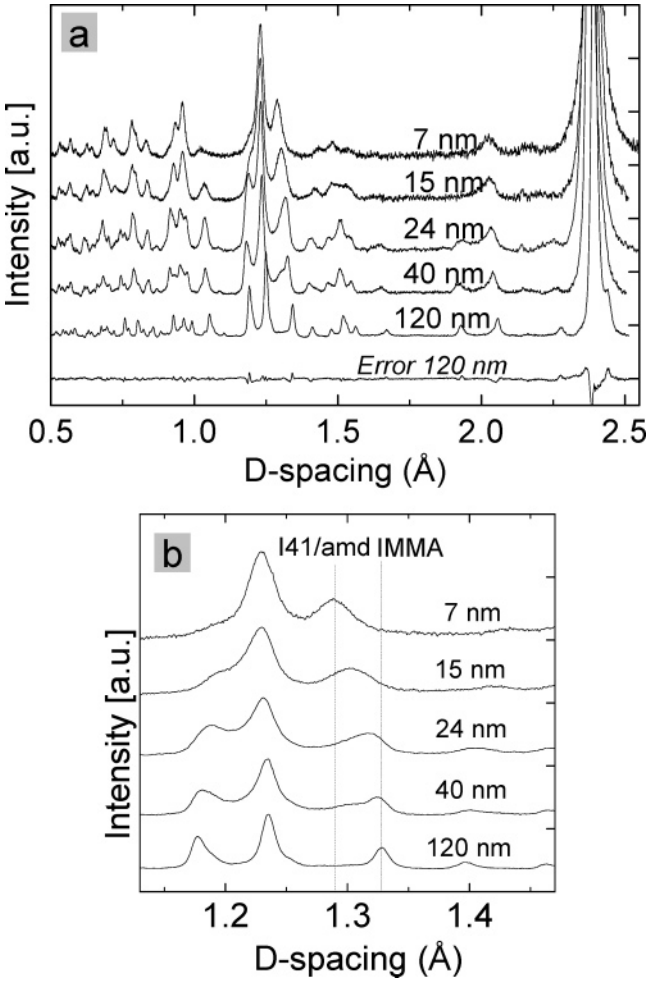

Figure 1. Neutron diffraction patterns of maximum lithiated Li_xTiO_2 for different particle sizes. (a) POLARIS (ISIS/UK) data (90° detector bank). (b) Detail indicating the crystallographic change from the orthorhombic (*Imma*) 120 nm material toward tetragonal (*I*41/*amd*) symmetry for the 7 nm material.

Table 1. Lattice Parameters and Space-Group for the Three Phases That Occur in Nanosized and Lithiated Anatase TiO_2

	space group	*a* (Å)	*b* (Å)	*c* (Å)
anatase	*I*41/*amd*	3.792	3.792	9.497
Li-titanate	Imma	3.819	4.084	9.066
Li_1TiO_2	*I*41/*amd*	4.043	4.043	8.628

The phase diagram of the composition versus the particle size shown in Figure 2, results from detailed Rietveld refinement of the data in Figure 1 and that of a range of other compositions (see Methods). A remarkable observation is that the Li-ion solubility in the various phases depends systematically on the crystal particle size. The 120 nm anatase crystals can host approximately Li/Ti = 0.03, similar to the anatase phase domains in microcrystalline particles.

However, 7 nm anatase particles are able to host up to Li/Ti = 0.21 while maintaining the anatase structure. This is in good agreement with the anatase solid solution domain in 6 nm crystal particles measured during electrochemical charging which extended up to $x = 0.22$.[4] Similarly the maximum observed Li content in the Li titanate phase increases with decreasing particle size, showing that for the smallest particle size a ~35% increase in the Li content of this phase can be realized.

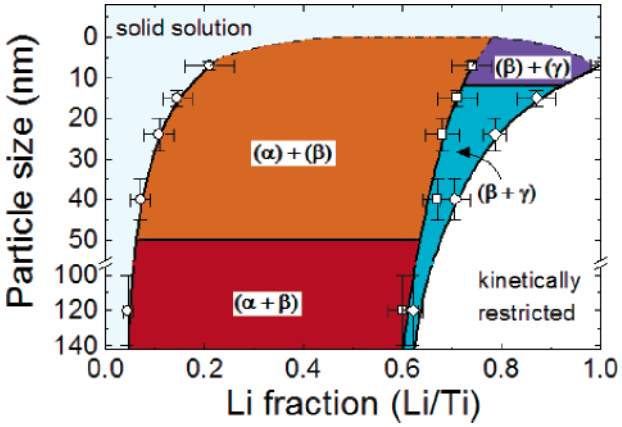

Figure 2. Phase diagram of the Li composition in anatase TiO_2 versus crystal particle size based on the neutron diffraction results. α indicates the anatase phase (*I*41/*amd*), β the Li-titanate phase (*Imma*) and γ the Li_1TiO_2 phase (*I*41/*amd*). The different notation of the phase coexistence, for instance (α+β) or (α)+(β), reflects respectively, the coexistence or non-coexistence of the two phases within one crystalline particle. The dashed lines are not experimentally probed and only represent a suggestion based on the results obtained for larger particles. The kinetically restricted domain reflects the poor ionic conductivity of the Li_1TiO_2 phase, which implies that particles larger than 7 nm cannot be fully transformed to this phase.

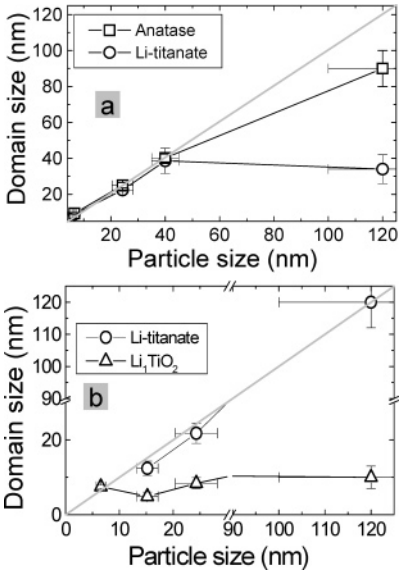

Figure 3. Domain sizes from neutron diffraction line broadening as a function of particle size. (a) For the individual anatase and Li-titanate crystallites that coexist and (b) for the Li-titanate and the Li_1TiO_2 phase coexistence in one particle.

A decrease in particle size raises the lithium capacity of the material considerably, due to the progressive formation of the Li_1TiO_2 phase (indicated as γ in Figure 2), ultimately leading to the theoretical maximum obtainable lithium fraction of $x = 1$ in 7 nm particles. Figure 2 indicates that electrochemical Li-insertion should lead to two two-phase regions: first the well-established anatase/Li-titanate (α/β) coexistence, and second the newly observed phase coexistence between Li-titanate and the Li_1TiO_2 phase (β/γ). This suggests the existence of a second voltage plateau upon (dis)charging in particular for small crystal particles. In 6 nm crystallites Sudant et al.[4] reach capacities that suggest the formation of the Li_1TiO_2 phase; however, a clear plateau could not be recognized. Possibly, this can be explained by the solid solution behavior in Li-titanate, and/or poor ionic conductivity of the Li_1TiO_2 phase, both discussed below.

Interestingly, a more evident second plateau is observed for micromaterial at elevated temperatures,[16,17] in line with the formation of the Li_1TiO_2 phase. The fact that microsized material can be transformed at elevated temperatures into the Li_1TiO_2 phase and not at room temperature indicates that the Li_1TiO_2 phase is a poor Li-ion conductor. The poor Li-ion conductivity can be due to the full occupation of the octahedral voids, whereas Li-ion diffusion requires vacancies. Most likely, the short diffusion path in nanostructured materials diminishes this problem, and as a consequence 7 nm particles (and smaller) can be fully transformed toward the Li_1TiO_2 phase, thereby reaching the theoretical capacity at room temperature. The slow diffusion in the Li_1TiO_2 phase averts the material to reach equilibrium within practical timescales for the composition/particle-size range indicated as kinetically restricted in Figure 2. (The part α and β part of the phase diagram must represent true equilibrium since the diffusion coefficients in the these phases[18,19] imply that equilibrium (after lithiation) is reached within minutes, whereas the materials were allowed to equilibrate for 3 days, see Methods). In conclusion, the Li_1TiO_2 phase rationalizes the increased capacity for smaller particle sizes reported in literature,[10−13,20,21] and the increased capacity of microsize particles at elevated temperatures.[16,17] The poor ionic conductivity of the Li_1TiO_2 phase also elucidates why at high (dis)charge rates only energy densities of less than $Li_{0.55}TiO_2$[6,22] are obtained.

In micron-sized crystal particles lithiation up to $x = 0.55$ causes the Li-titanate crystal phase to grow at the expense of the crystal anatase phase.[12] The growth of one phase at the cost of the other phase will cause the crystal domains size of both phases to vary with the overall composition. Consequently, the line-width broadening in the diffraction patterns as a function of composition will vary, as is indeed observed for microsized lithiated anatase.[12,18] However, the domain-size broadening in Figure 3(a) for the anatase and the Li-titanate phase for particles smaller than 120 nm shows that for both phases the domain size equals the particle size. Note that the particle size is used to indicate the pristine single-crystal particle size, and domain size to indicate a crystalline phase domain formed within a previously pristine single-crystal particle.

The only possible, but highly surprising, explanation is that a nanosized particle, smaller than 120 nm, has *either* the anatase *or* the Li-titanate phase. This indicates that the two phases do

(16) Zachauchristiansen, B.; West, K.; Jacobsen, T.; Atlung, S. Lithium Insertion in Different TiO_2 Modifications. *Solid State Ionics* **1988**, *28*, 1176−1182.
(17) Macklin, W. J.; Neat, R. J. Performance of Titanium Dioxide-Based Cathodes in a Lithium Polymer Electrolyte Cell. *Solid State Ionics* **1992**, *53*−*6*, 694−700.
(18) Wagemaker, M.; van de Krol, R.; Kentgens, A. P. M.; van Well, A. A.; Mulder, F. M. Two phase morphology limits lithium diffusion in TiO_2 (anatase): A Li-7 MAS NMR study. *J. Am. Chem. Soc.* **2001**, *123* (46), 11454−11461.
(19) Wagemaker, M.; Kentgens, A. P. M.; Mulder, F. M. Equilibrium lithium transport between nanocrystalline phases in intercalated TiO_2 anatase. *Nature* **2002**, *418* (6896), 397−399.
(20) Leroux, F.; Dewar, P. J.; Intissar, M.; Ouvrard, G.; Nazar, L. F. Study of the formation of mesoporous titania via a template approach and of subsequent Li insertion. *J. Mater. Chem.* **2002**, *12* (11), 3245−3253.
(21) Kavan, L.; Attia, A.; Lenzmann, F.; Elder, S. H.; Gratzel, M. Lithium insertion into zirconia-stabilized mesoscopic TiO_2 (anatase). *J. Electrochem. Soc.* **2000**, *147* (8), 2897−2902.
(22) Reiman, K. H.; Brace, K. M.; Gordon-Smith, T. J.; Nandhakumar, I.; Attard, G. S.; Owen, J. R. Lithium insertion into TiO_2 from aqueous solution - Facilitated by nanostructure. *Electrochem. Commun.* **2006**, *8* (4), 517−522.

not coexist within one particle with a size smaller than 120 nm, indicated as (α)+(β). Upon lithiation, of nanocrystalline particles smaller than 120 nm, simply more nanoparticles will be transformed toward Li-titanate, whereas in larger particles the Li-titanate phase domains grow within each particle at the expense of the anatase phase domains, indicated as (α+β).

In contrast the Li_1TiO_2 crystal phase domains coexists within one particle with the Li-titanate crystal phase domains, as can be deduced from the Li_1TiO_2 domain size shown in Figure 3(b) that is approximately constant for different particle sizes. Only the particles of 7 nm are completely transformed into the Li_1TiO_2 phase. Since lithium is inserted at the surface of the particles, it is reasonable to assume that the constant size of the Li_1TiO_2 crystal domains corresponds to a shell of constant width, surrounding the Li-titanate crystal core. The phase fractions resulting from Rietveld refinement of the fully lithiated materials (not shown) lead to a Li_1TiO_2 phase shell thickness of approximately 4 nm, independent of the particle size. This is smaller than indicated by the domain-size line broadening in Figure 3(b), because the shell shaped domain will lead to an effective domain size larger than the thickness of the shell. The conversion of only the first 4 nm of the materials toward the Li_1TiO_2 phase, irrespective of the particle size, is most likely the result of poor ionic conductivity, as discussed above, and is well in line with previous work where by means of surface sensitive reflection mode XAFS a 3−4 nm layer was identified having an effective Ti^{3+} oxidation state consistent with the Li_1TiO_2 composition.[23]

The horizontal lines in Figure 2 indicate the transition from phase coexistence within one particle, to a morphology where a particle is either one or the other crystal phase. The instantaneous conversion from one phase to the other was already suggested by *in situ* XRD on ~15 nm particles[24] and later for 40 nm Li_xTiO_2 particles.[25] Such instantaneous conversion is well recognized and understood for magnetic domains in small particles[26] and has recently also been theoretically suggested in binary alloys.[27] The coexistence of two magnetic domains, or two crystallographic phases within one particle leads to a domain wall-related energy penalty, where the latter will be determined by the strain mainly due to a difference in lattice parameters. In order to understand how a strain-induced energy penalty can destabilize the two-phase coexistence in small particles, we consider, ΔG_{mix}, the Gibbs free energy (per mole inserted Li ions) for mixing of two phases, 1 and 2, in a bulk material:

$$\Delta G_{mix}(x) = (x_2 - x_1)^{-1}((x_2 - x)G_1 + (x - x_1)G_2) - G(x) \qquad x_1 < x < x_2 \quad (1)$$

where x_1 and x_2 are the composition limits of the miscibility gap, G_1 and G_2 are the associated free energies in phases 1 and 2, respectively, and $G(x)$ is the free energy for the solid solution state. The first two terms represent the lowest two-point tangent with the free energy for a solid solution $G(x)$. The fact that $\Delta G_{mix}(x)$ is less than zero for $x_1 < x < x_2$ implies that phase separation is energetically more favorable. However, a phase boundary associated with phase coexistence will lead to a strain-induced energy penalty, which can be simply introduced as an effective increase of the molar Gibbs free energy for mixing:

$$\Delta G_{mix}(x) = (x_2 - x_1)^{-1}((x_2 - x)G_1 + (x - x_1)G_2) - G(x) + A(x)\gamma_A/(\nu_{Li}V) \qquad x_1 < x < x_2 \quad (2)$$

where $A(x)$ is the surface of the interface between the two phases 1 and 2, γ the surface energy due to strain, ν_{Li} the (inserted) Li-ion molar volume, and V the volume of the particle. Clearly, the last term will increase for smaller particle sizes, as the interface $A(x)$ will scale with r^2 and the volume with r^3, where r is the particle radius. As a result, the energy gain due to phase separation, represented by the free energy of mixing ΔG_{mix}, will decrease for smaller particle sizes. This will gradually close the miscibility gap for decreasing particle size, which explains the observed (see Figure 2) enhanced solubility of Li in the anatase phase for smaller particles. The increasing Li content in Li-titanate with decreasing particle size will depend on the stability of two two-phase equilibria (α/β and β/γ), and hence on the exact nature of the Gibbs free energy, which is outside the scope of this paper. Below a specific particle size, two-phase separation will be even thermodynamically ($\Delta G_{mix} > 0$ for $x_1 < x < x_2$) unstable within one particle, consistent with the disappearance of the phase coexistence observed for both $\alpha/\beta$and β/γ. The size of the surface energy, γ, determines at what particle size the phase coexistence disappears. The results in Figure 2 indicate that the surface energy for the anatase/Li-titanate interface is larger than that for the Li-titanate/Li_1TiO_2 interface. Currently, we are in the process of evaluating these effects in detail based on first principle calculations.

Considering the Gibbs free energy of one single particle, the disappearance of the phase coexistence within one particle, below 120 nm, suggests that the material can form a solid solution over the whole compositional range. However, in Figure 2 down to 7 nm a mixture of α and β particles is observed, i.e., not all particles have the same Li content but each particle is either α or β. In this way the material forms two phases without having phase boundaries within one particle, but with the particle surface effectively being the phase boundary. Similar to the interface energy, a surface strain relaxation energy term should be considered in eq 2. This is in line with Jamnik et al. who predicted that for small particles (in general <100 nm) the outer particle surface tension will affect the thermodynamics of insertion.[28] Here we suggest that this term may be responsible for the enhancement of the solid solution in the single-phased particles in the (α)+(β) region of Figure 2, following the same reasoning as above for the interface energy. Nevertheless, more research is required to establish the exact nature of these thermodynamics aspects of nanosizing.

Summarizing, the phase and particle boundary strain is introduced as a fundamental rationale to explain the observed

(23) Wagemaker, M.; Lutzenkirchen-Hecht, D.; van Well, A. A.; Frahm, R. Atomic and electronic bulk versus surface structure: Lithium intercalation in anatase TiO_2. *J. Phys. Chem. B* **2004**, *108* (33), 12456−12464.
(24) van de Krol, R.; Goossens, A.; Meulenkamp, E. A. In situ X-ray diffraction of lithium intercalation in nanostructured and thin film anatase TiO_2. *J. Electrochem. Soc.* **1999**, *146* (9), 3150−3154.
(25) Wagemaker, M. Borghols, W. J. H.; Eck, E. R. H.; Kentgens, A. P. M.; Kearley, G. J.; Mulder, F. M. The influence of size on phase morphology and Li-ion mobility in nano-sized lithiated anatase TiO_2. *Chem.-Eur. J.* **2006**, in press.
(26) Hubert, A., Schafer, R. *Magnetic domains: the analysis of magnetic microstructures*; Springer: Berlin, 1998.
(27) Johnson, W. C. Spinodal decomposition in a small radially stressed sphere. *Acta Mater.* **2001**, *49* (17), 3463−3474.
(28) Jamnik, J.; Maier, J. Nanocrystallinity effects in lithium battery materials - Aspects of nano-ionics. Part IV. *Phys. Chem. Chem. Phys.* **2003**, *5* (23), 5215−5220.

dramatic effects of particle size on the thermodynamics of insertion. Clearly, the influence of the phase boundary energetics on the thermodynamics of nanoparticles can be expected to be generally valid. Most likely, in any insertion material the difference in insertion reaction between bulk and nanomaterial is strongly influenced by the energetics of the phase boundaries. The present results suggest that, in general, nanosizing materials with a large phase boundary energy penalty (mostly true for materials with a large volume change upon insertion) will lead to the enhanced solid solution, and single-phased particle effects as observed at present for anatase TiO_2. In materials with practically no volume change upon insertion ("zero-strain" property), these effects upon nanosizing will be masked by the temperature-driven solid solution. The absence of the phase boundary-induced energy penalty leads to complete solid solution behavior for microsized particles already below room temperatures.[29]

Large practical implications will result because enhanced solid-solution behavior upon nanosizing is generally believed to lead to better interstitial dynamics, which in the case of Li ion and H storage leads to better output power densities of devices, additional to that resulting from the short diffusion path in nanocrystalline particles. This is relevant for various applications such as Li-ion batteries, hydrogen storage materials, and alloys involving interstitial carbon and hydrogen. Although the current results present the first systematic study on this effect, changes in the solubility of the inserted species upon nanosizing have also been reported for other materials. For nanosized $LiFePO_4$ there are indications that the Li-ion solubility depends on particle size,[30] which could be of considerable importance because stimulated solid solution behavior should improve the power density.[31,32] Similarly, in nanosized MgH_2 the phase behavior appears to be altered compared to the bulk material, leading to a $MgH_{0.8<x<2}$ solid solution region, which changes the storage kinetics dramatically.[33]

Conclusions

The structural results presented in this work show unambiguously that crystal particle size has a striking impact on the Li-insertion behavior. In general insertion materials with phase boundaries, the phase boundary energetics are likely to change the phase behavior dramatically, and the crystal particle size emerges as effective parameter to promote the solubility and solid solution behavior, as well as alter insertion capacities. This can be expected to have large impact on the kinetics and thermodynamics of insertion or intercalation reactions, which is of practical relevance in many technologically important materials.

Acknowledgment. This work is a contribution from the Delft Institute for Sustainable Energy (DISE). Financial support from The Netherlands Organization for Scientific Research (NWO) for the CW-VENI grant to M.W. and neutron beam time at ISIS are gratefully acknowledged. We thank N. H. van Dijk for fruitful discussions, Ron Smith and Steve Hull for assistance with the neutron diffraction measurements at POLARIS (ISIS), and Ugo Lafont for performing TEM measurements.

JA067733P

(29) Wagemaker, M., S. D. l. R., Kelder, E. M.; Schoonman, J.; Ringpfeil, C.; Haake, U.; Lützenkirchen-Hecht, D.; Frahm, R.; Mulder, F. M. A Kinetic Two-Phase and Equilibrium Solid Solution in Spinel $Li_{4+x}Ti_5O_{12}$. *Adv. Mater.* **2006**, *18* (23), 3169−3173.

(30) Yamada, A.; Takei, Y.; Koizumi, H.; Sonoyama, N.; Kanno, R.; Itoh, K.; Yonemura, M.; Kamiyama, T. Electrochemical, magnetic, and structural investigation of the $Li_x(Mn_yFe_{1-y})PO_4$ olivine phases. *Chem. Mater.* **2006**, *18* (3), 804−813.

(31) Delacourt, C.; Poizot, P.; Tarascon, J. M.; Masquelier, C. The existence of a temperature-driven solid solution in Li_xFePO_4 for $0 \leq x \leq 1$. *Nat. Mater.* **2005**, *4* (3), 254−260.

(32) Yamada, A.; Koizumi, H.; Nishimura, S. I.; Sonoyama, N.; Kanno, R.; Yonemura, M.; Nakamura, T.; Kobayashi, Y. Room-temperature miscibility gap in Li_xFePO_4. *Nat. Mater.* **2006**, *5* (5), 357−360.

(33) Schimmel, H. G.; Huot, J.; Chapon, L. C.; Tichelaar, F. D.; Mulder, F. M. Hydrogen cycling of niobium and vanadium catalyzed nanostructured magnesium. *J. Am. Chem. Soc.* **2005**, *127* (41), 14348−14354.